Syntax without Language: Neurobiological Evidence for cross-domain syntactic computations

Marco Tettamanti[1,2,3,CA], Irene Rotondi[4], Daniela Perani[1,2,3,4,6], Giuseppe Scotti[2], Ferruccio Fazio[1,5,6], Stefano F. Cappa[2,3,4], and Andrea Moro[2,3].

[1]Division of Neuroscience, San Raffaele Scientific Institute, Milano, Italy; [2]CERMAC-HSR, Milano, Italy; [3]National Institute of Neuroscience, Torino, Italy; [4]Vita-Salute San Raffaele University, Milano, Italy; [5]Università Milano-Bicocca, Monza (MI), Italy; [6]Institute of Molecular Bioimaging and Physiology, CNR, Segrate (MI), Italy.

[CA] Corresponding author:

Marco Tettamanti, Ph.D., San Raffaele Scientific Institute, Via Olgettina 58, I-20132 Milano, Italy, Tel ++39-02-26434888, Fax ++39-02-26434892; Email: tettamanti.marco@hsr.it

ABSTRACT

Not all conceivable grammars are realized within human languages. Rules based on *rigid* distances, in which a certain word must occur at a fixed distance from another word, are never found in grammars of natural languages. Distances between words are specified in terms of relative, *non-rigid* positions. The left inferior frontal gyrus (Broca's area) has been found to be involved in the computation of non-rigid but not of rigid syntax in the language domain. A fundamental question is therefore whether the neural activity underlying this non-rigid architecture is language-specific, given that analogous structural properties can be found in other cognitive domains. Using event-related functional magnetic resonance imaging in sixteen healthy native speakers of Italian, we measured brain activity for the acquisition of rigid and non-rigid syntax in the visuo-spatial domain. The data of the present experiment were formally compared with those of a previous experiment, in which there was a symmetrical distinction between rigid and non-rigid syntax in the language domain. Both in the visuo-spatial and in the language domain, the acquisition of non-rigid syntax, but not the acquisition of rigid syntax, activated Brodmann Area 44 of the left inferior frontal gyrus. This domain-independent effect was specifically modulated by performance improvement. Thus, in the human brain, one single "grammar without words" serves different higher cognitive functions.

Keywords: Broca's area; fMRI; Hierarchical; Syntactic; Visuo-spatial.

1. INTRODUCTION

Can a human grammar exist without words? The fundamental question we address here is whether syntax, a core aspect of the highly integrated system of universal properties that form the grammar of any human language, is subserved by a language-specific neural organization or not (Hauser et al., 2002; Tettamanti et al., 2002; Marcus et al., 2003; Tettamanti and Weniger, 2006). In all natural languages the syntactic dependencies are established on the basis of the hierarchical phrase structure generated by recursive rules rather than by the linear order of words (Chomsky, 1957). The conclusion that syntactic dependencies are based on recursive phrase structure is corroborated by the fact that there is no human language where a certain word must occur at a fixed distance from another (Chomsky, 1956). Distances between words are specified in terms of relative position and they can always be recursively expanded. For example, within noun phrases, the distance between an adjective and a noun can vary, such as in “a horrible flu”, “a horrible nasty flu”, “a horrible nasty bad flu”. Of course, this does not apply to idioms, such as in "kick the bucket" where "bucket" always follows "kick" after one word. But notice that, in this case, the complex "kick the bucket" is arguably not formed via a recursive procedure. In fact, it is invisible to transformation, such as passive: *"the bucket was kicked by John". Thus, idioms can be considered on a par with compounds, where the words forming the compound are displayed at a fixed order, such as in “blackboard”. Therefore, “non-rigid” syntactic dependencies (NRSD) – i.e. syntactic rules established between words at varying positions – consitute the core type of dependencies found in the syntax of all natural languages. Their counterparts, “rigid” syntactic dependencies (RSD) – i.e. syntactic rules established between words at fixed positions – are never found in human languages (Figure 1A).

It is worth noting that, within the so-called Minimalist Program of research in linguistics (Chomsky, 1995), the idea that all components of grammar are domain specific has been abandoned (Hauser et al., 2002). NRSD, at least in simple form, are not unique

to language; parallels can be found in other cognitive domains, including music (Patel, 2003), action control (Greenfield, 1991; Conway and Christiansen, 2001), and visuo-spatial processing (Greenfield, 1991). These instances of sequential behavior also rely on hierarchical cognitive control and structuring (Lashley, 1951; Greenfield, 1991; Byrne and Russon, 1998). These control mechanisms are required for manageability of complexity, sequence and outcome predictions, and repair; they consist in organizing simple subunit-chunks into higher order assemblies of increasing hierarchical complexity (Byrne and Russon, 1998; Conway and Christiansen, 2001). The grouping of elements into subunit-chunks according to feature and contextual similarity and the linkage of subunits into more complex hierarchical structures, are both flexible processes based on relative (non-rigid) rather than fixed sequential dependencies (Conway and Christiansen, 2001). Several types of evidence concur in suggesting that common, basic neural and computational mechanisms may underlie both language and non-linguistic sequential processing (see Tettamanti, 2003 for a review). With respect to parallels between language and visuo-spatial processing, a relevant observation is that visuo-spatial skills are employed in processing rigid and non-rigid arrays of abstract elements such as symbols. Aphasic patients with damage to Broca's area that show a lack of hierarchically organized syntactic production have been reported to also be impaired in drawing hierarchically organized tree structures (Grossman, 1980; Greenfield, 1991). Similarly, agrammatic aphasics have been found to be impaired in the processing of rule-based non-linguistic letter sequences (Dominey et al., 2003). Neurophysiological studies employing a similar task in healthy subjects found comparable left anterior negativity effects for the processing of both linguistic and non-linguistic rule-based sequences (Hoen and Dominey, 2000). Accordingly, both linguistic and non-linguistic rule-based sequences were found to activate the frontolateral cortex, bilaterally, in a functional magnetic resonance imaging (fMRI) study (Hoen et al., 2006).

Here we propose that the core properties characterizing NRSD are encoded by the

human brain independent of the cognitive domain in which they occur. To test this hypothesis, at least two pieces of evidence need to be collected. First, it has to be shown that NRSD, as the only type of syntactic dependencies found in natural languages, elicit unique brain responses compared to RSD. Second, by symmetrically comparing NRSD and RSD in non-linguistic cognitive domains, NRSD specific brain responses overlapping with those found for language must be observed. The first type of evidence has been previously provided, relying on works (Embick et al., 2000; Moro et al., 2001) that disentangle the neural basis of syntax from other linguistic components. The acquisition of grammatical rules governed by NRSD versus RSD was shown to depend on the activation of the *pars opercularis* of the left inferior frontal gyrus (IFG), which is part of the anatomical region traditionally defined as Broca's area (Tettamanti et al., 2002; Musso et al., 2003). In the study by Tettamanti and colleagues (2002), native speakers of Italian acquired novel syntactic rules reflecting NRSD versus RSD during fMRI acquisitions. The novel syntactic rules were generated by selectively manipulating word order in a synthetic version of Italian, in which open-class word roots were replaced by pseudowords. In the fMRI study by Musso and colleagues (2003), native speakers of German were taught Italian and Japanese, including natural NRSD rules and invented RSD rules. Specific effects for both Italian and Japanese showed that the left IFG selectively responded to NRSD across a wide-range of typological grammatical variations. More recently, Broca's area has been shown to selectively subserve the processing of hierarchical dependencies compatible with NRSD, as opposed to local transitions compatible with RSD, which solely depend upon the left frontal operculum, i.e. the cortical band between the crown of the *pars opercularis* in the left IFG and the anterior insula (Friederici et al., 2006). In the present experiment we searched for the second, stronger, type of evidence, i.e. we predicted that the left IFG is modulated by the acquisition of NRSD also in non-linguistic domains.

To this purpose, we performed an fMRI experiment that is symmetric to our previous experiment on the acquisition of syntactic rules (Tettamanti et al., 2002). There, we used a

word-based syntax to contrast the acquisition of NRSD (experimental condition word-NRSD) and RSD (experimental condition word-RSD) in the language domain. In the present experiment we used a symbol-based syntax to contrast the acquisition of NRSD (experimental condition symbol-NRSD) and RSD (experimental condition symbol-RSD) in the visuo-spatial domain (Figures 1B,C). The symmetrical experimental design allowed us to formally compare the data of the two experiments. The results demonstrated that, both in the language and in the visuo-spatial domain, the acquisition of rules based on NRSD, but not of rules based on RSD, depends on the left IFG.

2. METHODS

2.1 Subjects

Sixteen right-handed volunteer subjects (8 females, mean age 23.0 years, range 19-31 years) of comparable education level (Graduate Level) took part in the experiment. They were all native monolingual speakers of Italian, with no history of neurological or psychiatric disorders and no structural brain abnormalities. Participants also lacked any knowledge or familiarity with written or spoken Korean or with any other non-Indoeuropean language. They gave written consent to participate in the study after receiving an explanation of the procedures. The study was approved by the Ethics Committee of the San Raffaele Scientific Institute, Milano, Italy.

2.2 Experimental design

Participants viewed sequences of strings made of symbols that mimicked simple syntactic relations. These relations were characterized by agreement between two symbols either at varying positions (symbol-NRSD) or at fixed positions (symbol-RSD). Symbol-NRSD rules were equal to symbol-RSD rules in all respects, except for an

additional degree of freedom that allowed symbols governed by NRSD to occur at varying positions (Figure 1B). Participants acquired these syntactic relations during fMRI data collection by inferring them from the regularities in the sequences of strings.

2.2.1 Norms

The experimental design, including the choice of symbols and stimuli (strings), was optimized prior to fMRI scanning based on a norm on 24 healthy subjects, and was then tested in its final version on a further norm on 12 healthy subjects.

2.2.2 Symbols

In order to minimize a possible bias of subvocal verbalization (as would have been the case for instance with roman alphabet letters or simple geometrical shapes such as circles or triangles), we chose a set of 10 symbols (henceforth termed k1, k2, ... k10), slightly adapted from the Hangul Korean alphabet. The 10 symbols had characteristic shapes which made the distinction among them easy (all symbols are labelled and visible at least once in Figure 1B), but none of the shapes could be easily and consistently associated with common objects or entities. The symbols had 4 different colors (blue, green, red, yellow) and 2 different sizes (small vs. large) allowing agreement to be established.

2.2.3 Stimuli (strings)

Strings ranged in length between 3 and 7 symbols. The length of strings was balanced across experimental conditions. The experimental conditions were non-rigid syntactic dependencies (symbol-NRSD), rigid syntactic dependencies (symbol-RSD), and one baseline. In symbol-NRSD, two symbols of different shape agreed by color and size, and their position varied freely (rule symbol-NRSD-1: k1 and k2 had the same color, were large and their position varied freely (see example strings *NRi*, *NRii*, and *NRiii* in Figure

1B, left); rule symbol-NRSD-2: k3 and k4 had the same color, were large and their position varied freely (not shown)). In symbol-RSD, two symbols of different shape agreed by color and size, but their position was fixed (rule symbol-RSD-1: k1 and k2 had the same color and were large; k1 was in 1st and k2 in 3rd position (see example strings *Ri*, *Rii*, and *Riii* Figure 1B, right); rule symbol-RSD-2: k3 and k4 had the same color and were large; k3 was in 1st and k4 in 3rd position (not shown)). In both symbol-NRSD and symbol-RSD, all other symbols were small and of random shape and color. In the baseline, all symbols within a string were small and equal in shape, except for one symbol which was large and had a different shape (e.g. 'k5 k6 k5 k5 k5'). Such a simple baseline rule (as opposed to e.g. fully randomized strings of symbols) was conceived in order to maximally eliminate rule inference processes from the baseline (see also Task instructions).

For symbol-NRSD and symbol-RSD, incorrect strings may consist of either i) one of the two target symbols missing, or ii) two symbols having the same color and a large size that were not the target symbols (e.g. k7 and k8 instead of k1 and k2; see also Figure 1C). For symbol-RSD only, incorrect strings may also consist of target symbols at incorrect positions (e.g. k1 in 2nd position). Thus, the acquisition of symbol-RSD versus symbol-NRSD required the fixation of an additional degree of freedom (i.e. position). In other words, in symbol-RSD the position of the target symbols did not vary freely. Incorrect strings for the baseline consisted of symbols that were all small and equal in shape.

2.2.4 Task

Participants underwent 8 event-related functional scanning sessions each, 4 with the baseline task, and 4 introducing a novel rule each (either symbol-NRSD-1, symbol-NRSD-2, symbol-RSD-1, or symbol-RSD-2). The order of sessions was counterbalanced across participants. Task sequences during scanning sessions consisted of a short, initial block (sample block), in which 5 correct strings were presented. The sample block was followed by a longer block (probe block) of 56 strings, 50% correct and 50% incorrect.

Correct and incorrect strings were randomly intermixed. Each string was only presented once to each participant. Strings appeared at the centre of the visual field and were kept displayed until a response key was pressed (self-paced event-related design). During the sample block, participants passed from one string to the next by pressing the left response key with their right index. During the probe block, participants pressed the left response key with their right index finger if they judged that the string was correct, and the right key with their right middle finger if they judged that the string was incorrect. A feedback indicating a right or wrong answer appeared for 500 msec immediately after response. In case of a wrong answer, an additional new sample (correct) string was presented, after which the probe block was resumed. Intervals between trials – i.e. between the participant's response (sample blocks) or the end of the feedback presentation (probe blocks) and the presentation of the next string – corresponded to three different durations, i.e. 1158 msec, 2073 msec, and 2964 msec (randomly ordered, in the proportion 4:2:1; Figure 1C). Intervals of varying durations were used to maximise the haemodynamic signal sensitivity of the event-related design (Dale, 1999). Over all participants and experimental conditions, the average trial duration was 3131 msec (st. dev. = 678 msec), inclusive of self-paced stimulus duration, feedback and variable interval (symbol-NRSD: mean = 3162 msec, st. dev. = 736 msec; symbol-RSD: mean = 3263 msec, st. dev. = 718 msec; Baseline: mean = 2970 msec, st. dev. = 484 msec).

In the baseline task, the rule was explicitly pre-specified to participants, in order to avoid rule inference processes. In symbol-NRSD and symbol-RSD, rules were not made explicit, and subjects were asked to infer them from the regularities characterizing the strings across each task session. After the end of each scanning session, the participants were asked to verbally describe the rule they had just learned. All participants were able to provide comprehensive rule definitions that captured all relevant rule parameters.

2.2.5 Task instructions

The task instructions were given to the volunteers in written form and were as follows. A sample string containing randomly arranged symbols differing by shape and color was presented on top of the page. Subjects were instructed that they had to perform two distinct tasks based on sequences of such strings. “In the one [baseline] task, correct strings will contain symbols which are all small and equal in shape, except for one symbol which is large and has a different shape. A brief instruction will prompt a short sample block consisting of correct strings only. You shall watch each string carefully and once you are finished press the left response key with your right index finger. Subsequently, another instruction will prompt a probe block consisting of correct strings conforming to those presented in the sample block which will be intermixed with incorrect strings, i.e. strings containing symbols which are all small and equal in shape. If you think that the string conforms to those presented in the sample block, you shall press the left response key with your right index finger, otherwise you shall press the right key with your right middle finger. Feedback for correct and incorrect responses will be provided. In case of an incorrect answer, a new correct sample string will be presented, after which the probe block will be resumed. The other [rule learning; the distinction between symbol-NRSD and symbol-RSD was never made explicit] task will be structured in exactly the same manner. However, in this case you shall infer the rule governing correct strings by yourself, based on the sample block, which consists of correct strings only, based on the feedback received in the probe block, and on the new correct strings presented in case of an incorrect response.”

2.2.6 Task familiarization

Before positioning in the magnet, participants were given one short baseline, and one short learning sequence for familiarization with the tasks (both with a sample block of 5 strings and a probe block of 28 strings). In the familiarization baseline sequence, we used exactly the same pre-specified rule as for fMRI scanning. In the familiarization

learning sequence, the rule was that strings were exclusively formed by large k7, all of the same color (e.g. k7 k7 k7 k7), and incorrect trials could be any violation of this rule (i.e. different colors or different symbols).

2.2.7 Stimulation hardware and software

Stimuli were presented with Presentation 0.91 (Neurobehavioral Systems, Albany, CA, USA), and viewed via a back-projection screen located in front of the scanner and a mirror placed on the head coil. Behavioral responses (accuracy and speed) were collected via a fiber-optic response box during task execution in the MR scanner.

2.2.8 Performance index

For the analysis of behavioral responses, we developed a performance index (PI) as a continuous variable (in percent units) that takes into account both reaction times and accuracy, according to the formula: PI(n) = 100 – ({[(%errors(n)+1)*RT(n) – GrandMin] / GrandMax} * 100); n is the n^{th} stimulus; %error(n) is the percentage of errors in the interval from n-5 to n+4 (i.e. the performance at the n^{th} stimulus is a function of the stability of the accuracy over preceding and subsequent stimuli: a correct response corresponds to a higher PI when the preceding and subsequent responses were on average correct than when they were on average wrong; the rationale underlying this choice is that the probability that correct responses are due to correct rule inference rather than to chance is higher when no errors occur during a prolonged interval); RT(n) is the reaction time for the n^{th} stimulus; GrandMin and GrandMax are the minimum and the maximum value of [%errors(n)+1)*RT(n)] respectively, over all responses of all the participants. In other words, a PI(n) = 100 indicates that the n^{th} stimulus was processed with maximal speed and accuracy, whereas a PI(n) = 0 indicates minimal speed and accuracy. The use of a PI, as opposed to the separate analysis of accuracy and reaction times (but see Tables 3A,B), was motivated by the nature of the experimental design (self-paced task with explicit

feedback) that minimizes speed-accuracy trade-off effects. We also checked that the use of a PI did not cause any loss of relevant information in the fMRI data analysis.

2.3 Statistical analysis of behavioral data

Non-parametric tests (Table 2) were used due to the nonnormal distribution of PI behavioral data. For the purpose of the statistical analysis of behavioral data, the data points over task duration were grouped in 8 blocks of 14 responses (both correct and incorrect) each (block1: responses to strings 1-14; block2: responses to strings 15-28; ... block8: responses to strings 99-112). For each experimental condition, the first 4 blocks corresponded to the scanning session that was presented first in the randomization order, the last 4 blocks to the second scanning session (Figure 4C). In order to have balanced data sets across conditions, for the baseline condition we only included the first two scanning sessions (no significant differences were found between the first two sessions and the last two sessions for the Baseline condition). Only the responses to the strings of the probe blocks were considered (56 per session). We performed a Kruskal-Wallis test (n=16) with task (3 levels: baseline, symbol-NRSD, symbol-RSD) and block (8 levels: blocks 1-8) as independent factors and PI as the dependent variable. We also performed Wilcoxon paired tests (n=16) between the 3 levels of the task factor and between block1 and block8 of each condition. In order to make sure that the use of PI did not lead to spurious effects, we also performed the same analysis on reaction times and accuracy data, separately (see Tables 3A,B).

2.4 fMRI data acquisition

MRI scans were acquired on a 3T Intera Philips body scanner (Philips Medical Systems, Best, NL) using an 8 channels-sense head coil (sense reduction factor = 2). Whole-brain functional images were obtained with an echo-planar T2*-weighted gradient-echo sequence, using blood-oxygenation-level-dependent contrast. Each functional image

comprised 30 contiguous axial slices (4 mm thick), acquired in interleaved mode, and with a repetition time of 3000 msec (acquisition time: 1700 msec; echo time: 30 msec; field of view: 240 mm x 240 mm; matrix size: 128 x 128; flip angle 85°). Each participant underwent 8 functional scanning sessions of 408 sec duration (corresponding to 136 scans, preceded by 5 dummy scans that were discarded prior to data analysis).

2.5 fMRI data analysis

Statistical parametric mapping (SPM2, Wellcome Department of Imaging Neuroscience, London, UK) was used for slice timing, image realignment and unwarping (Andersson et al., 2001), normalization to the Montreal Neurological Institute (MNI) standard space, smoothing by a 6 mm FWHM Gaussian kernel, and statistical analysis (Friston et al., 2002). We adopted a two-stage random-effects approach (Penny and Holmes, 2003) to ensure generalizeability of the results at the population level (Frison and Pocock, 1992).

2.5.1 First-level statistical models

At the first stage, the time series of each participant were high-pass filtered at 67 sec and pre-whitened by means of an autoregressive model AR(1) (Andersson et al., 2001). Global differences in fMRI signal were compensated using proportional scaling; global scaling was chosen to eliminate between-sessions confounds from the comparisons between experimental conditions, given that each session only comprised one experimental condition. Haemodynamic evoked responses for all experimental conditions were modeled as Finite Impulse Responses (Henson, 2003), consisting in trains of 8 contiguous box-car functions of 3 sec duration each (post-stimulus time bins, cfr. Figure 2C), with the onset of each train corresponding to stimulus appearance (Figure 1C). A Finite Impulse Response model was chosen to account for the non-canonical sustained responses associated with the self-paced learning task (cfr. Figure 2C).

Three independent effects were evaluated at the single-subject level: *a*) Overall task effects, looking for global effects of experimental conditions, where we modelled the NRSD, RSD, and baseline regressors; *b*) Parametric modulation in time, allowing to assess learning related changes, i.e. temporal changes of activation across scans, independently from the overall task effects and from the individual differences in learning rate measured by PI; *c*) Parametric modulation induced by changes in behavioral performance, i.e. learning related changes of activation correlating with changes in PI, independently from the overall task effects and from time.

We specified a set of t-Student contrasts corresponding to these three separate effects, which were then fed into the second-level statistical models.

2.5.2 Second-level statistical models

At the second stage of analysis, the contrast images obtained at the single-subject level were used to compute a set of ANOVAs assessing their significance at the group-level (n = 16 participants). All reported effects relate to voxel-level statistics and survived a $p < .05$, false discovery rate (FDR) error type correction for multiple comparisons (see below, section *2.5.3*). We evaluated the three independent effects ensuing from the first-level analysis:

a) Overall task effects

Within this analysis we computed a conjunction effect between symbol-NRSD and symbol-RSD (Table 1A, Figure 2A), using the conjunction null hypothesis (Nichols et al., 2005). The conjunction was calculated in two distinct ways: in a first pass, we calculated the conjunction with weights convolved with the haemodynamic response function (Henson, 2003), to account for canonical response shapes in visual areas (blue areas in Figure 2A); in a second pass, we calculated the conjunction by equally weighting all eight post-stimulus time bins of each condition, to account for sustained responses (yellow areas in Figure 2A). Within this analysis, we also computed the two condition-specific

interactions (Table 1B, Figure 2C), i.e. [(symbol-NRSD – Baseline) – (symbol-RSD – Baseline)] and [(symbol-RSD – Baseline) – (symbol-NRSD – Baseline)]. For further confidence in the results yielded by the condition-specific interactions, we also ensured that qualitatively similar results were obtained by the two simple main effects ([(symbol-NRSD – Baseline)] and [(symbol-RSD – Baseline)], see Table 1b).

b) Parametric modulation in time

Here we assessed the condition-specific, learning-related temporal changes of activation across scans in symbol-NRSD versus symbol-RSD, i.e. time x tasks interactions (Figure 3).

c) Parametric modulation induced by changes in behavioral performance

Here we assessed the condition-specific, learning-related changes of activation correlating with changes in performance in symbol-NRSD versus symbol-RSD, i.e. performance x tasks interactions (Figure 4).

2.5.3 Commonalities between word syntax and symbol syntax acquisition (small volume correction procedure)

A crucial aim of the present experiment was to assess the overlap between the areas of activation associated with symbol-NRSD and symbol-RSD and the areas found to be active in our previous experiment with linguistic material (Tettamanti et al., 2002). In that experiment, the difference between the two main conditions was isomorphic to symbol-NRSD and symbol-RSD conditions but it involved words rather than strings of symbols (conditions word-NRSD and word-RSD). To find areas that were activated by word syntax acquisition and were also activated by symbol syntax acquisition, a small volume correction for multiple comparisons ($p < .05$, FDR error type correction) was adopted for all the contrasts of the analysis of the overall task effects and of the temporal and behavioral parametric modulations. This restricted the analysis to a mask including those voxels which were significant in the main effect of word-NRSD and word-RSD (p

< .05, FDR corrected). The effects that survived this small volume correction procedure represent areas of anatomo-functional coincidence between symbol and word syntax and are marked by a ‡ index in Tables 1A,B. The effects that did not survive the small volume correction procedure (but survived a p < .05, FDR correction over the entire brain volume of acquisition) represent areas that are only activated by symbol syntax and are indicated by a § index in Tables 1A,B.

2.5.4 Anatomical mapping of functional data

We assessed the cytoarchitectonic probability of activations in the left IFG, using the probability maps (Amunts et al., 1999) for BA 44 and BA 45 available with the SPM Anatomy toolbox (http://www.fz-juelich.de/ime/spm_anatomy_toolbox). For anatomical localization and visualization of brain activations, we acquired 2 high-resolution whole-brain structural T1 weighted scans (resolution 1mm x 1mm x 1mm) of each participant, following the functional scanning sessions. We used SPM2 for coregistering the 2 structural scans of each participant, averaging the two coregistered scans, and normalizing the average structural image to the MNI standard space. We then averaged the normalized structural images of the 16 participants in one single image. This average structural image was automatically segmented with SureFit 4.45 to obtain a cortical surface reconstruction with tissue specific image values for sulcal versus gyral cortex (Van Essen et al., 2001). Caret 5.2 was used for flat maps generation, and to map brain activations obtained with SPM2 and cytoarchitectonic probability maps onto cortical surface maps (Van Essen et al., 2001).

3. RESULTS

The analysis of fMRI data sought for overall task effects, learning-related parametric modulation of these effects in time, and parametric modulation induced by learning-related

changes in behavioral performance.

3.1 Overall task effects

A conjunction analysis looking for canonical haemodynamic responses showed that both symbol-NRSD and symbol-RSD activated extrastriate visual areas, bilaterally. A second conjunction analysis looking for sustained haemodynamic responses showed that both symbol-NRSD and symbol-RSD activated the right frontolateral cortex, and a bilateral network involving parietal areas, and the anterior cingulate gyrus. We then compared the results of the present experiment with those of our previous experiment (Tettamanti et al., 2002) by using a small volume correction procedure. This procedure showed that the activation of extrastriate visual areas, including the inferior and middle occipital gyri and the fusiform gyrus, bilaterally, was only found for symbol syntax acquisition; conversely, the other brain regions were activated in symbol syntax acquisition in the same way as in word syntax acquisition (Table 1A, Figures 2A,B).

In addition, we tested for specific activations for symbol-NRSD and symbol-RSD, respectively, by using interaction contrasts that reveal higher signal increases for one rule type vs. the other with respect to the baseline condition. The interaction effects showed that both symbol-NRSD and symbol-RSD activated the left IFG but in anatomically segregated sub-regions, whereas only symbol-RSD activated the right IFG (Table 1B, Figure 2C). In the left IFG, the activation with a higher response for symbol-NRSD than for symbol-RSD was attributed to Brodmann area (BA) 44, whereas the activation with a higher response for symbol-RSD than for symbol-NRSD was attributed to BA 45, according to cytoarchitectonic probability maps (Amunts et al., 1999) (Figure 2D). The small volume correction procedure showed that the anatomical location of both activations in the left IFG (BA 44 and 45) coincided with the location of the corresponding activations found for word syntax acquisition.

3.2 Parametric modulation in time

An analysis of parametric modulation allowed us to detect learning-related temporal changes of activation during symbol syntax acquisition. The time x tasks interaction showed that the *pars opercularis* within the left IFG (Z score = 2.48; k = 11; x,y,z (mm) = -58, 14, 28; 60% probability of being left BA 44) was modulated in time in symbol-NRSD significantly more than in symbol-RSD (Figures 3A,B). The anatomical location of this effect was compared to that of word syntax acquisition (x,y,z (mm) = -60, 8, 16; 40% probability of being left BA 44) via the small volume correction procedure: for this particular type of analysis only (parametric modulation in time), although an activation in BA 44 was found in both experiments, the locations of the two activations did not coincide. No other brain regions showed a significant effect, neither for symbol-NRSD nor for symbol-RSD.

3.3 Parametric modulation induced by changes in behavioral performance

All the participants acquired the novel rules of symbol syntax and attained a high proficiency (symbol-NRSD: mean PI = 99.05, st. dev. = 3.01; symbol-RSD: mean PI = 97.15, st. dev. = 5.34; Baseline: mean PI = 99.65, st. dev. = .45). In both symbol-NRSD and symbol-RSD there was a significant improvement in response accuracy and speed, as reflected in changes of performance index (PI) over blocks, compared to the baseline task. We also found a significant difference in PI between symbol-NRSD and symbol-RSD: symbol-RSD were acquired more slowly, although a proficiency level comparable to symbol-NRSD was attained by the end of the scanning sequences (Table 2, Figure 4C). Errors in symbol-RSD were mainly for incorrect strings with target symbols at incorrect positions, compatible with the need to fixate an additional degree of freedom (i.e. position). The average scores at block 1 were: symbol-NRSD: mean PI = 97.31, st. dev. = 5.95; symbol-RSD: mean PI = 91.99, st. dev. = 8.38; Baseline: mean PI = 99.38, st. dev. = .67. The average scores at block 8 were: symbol-NRSD: mean PI = 99.51, st. dev. = .63;

symbol-RSD: mean PI = 99.42, st. dev. = .72 ; Baseline: mean PI = 99.85, st. dev. = .16.

In order to make sure that the use of PI, as a summary measure that takes into account both reaction times and accuracy, did not lead to spurious effects, we also report the results of the separate analysis of reaction times and accuracy behavioral data. These results were largely comparable to those described above for PI (Tables 3A,B).

To assess learning-related changes of activation induced by changes in behavioral performance, we assessed parametric modulation of haemodynamic responses by PI. Despite a greater difficulty in acquiring symbol-RSD rules, the *pars opercularis* within the left IFG (Z score = 2.25; k = 15; x,y,z (mm) = -54, 12, 24; 50% probability of being left BA 44) presented a greater modulation in symbol-NRSD than in symbol-RSD (Figures 4A,B). In other words, the subtle improvement in PI of symbol-NRSD elicited a stronger signal change in the left IFG than the relatively more pronounced improvement in PI of symbol-RSD. A greater modulation of the right hemispheric homotopic area (Z score = 2.45; k = 11; x,y,z (mm) = 50, 18, 16; 50% probability of being right BA 44) in symbol-RSD than in symbol-NRSD was also found (Figure 4A). The small volume correction procedure showed that the anatomical location of the activations in both the left IFG and the right IFG coincided with the location of the corresponding activations found for word syntax acquisition. No other brain regions showed a significant effect.

Taken together, the behavioral and imaging data allows one to exclude that the differences in activation of the left IFG between symbol-NRSD and symbol-RSD, included those observed in the other two types of analyses described above, were merely due to a hypothetical greater difficulty in acquiring symbol-NRSD versus symbol-RSD. Symbol-RSD were actually acquired more slowly than symbol-NRSD: this is in agreement with our predictions, based on the fact that the acquisition of symbol-RSD versus symbol-NRSD required the fixation of an additional degree of freedom (i.e. position).

3.4 Summary of results

In summary, the bilateral fronto-parietal network engaged by the acquisition of symbol based syntax was largely equivalent to the network engaged by the acquisition of word based syntax. Crucially, also in the visuo-spatial domain, the acquisition of rules based on NRSD, but not of rules based on RSD, depended on the activation of BA 44 in the left IFG.

4. DISCUSSION

According to classical neuropsychology, linguistic and visuo-spatial functions are subserved by complementary neural representations with, in right-handers, linguistic functions predominantly represented in the left hemisphere and visuo-spatial functions predominantly represented in the right hemisphere. The basis of this hemispheric specialization is still controversial (Hugdahl and Davidson, 2003). The nature of the task, more than the nature of the stimuli, appears to be responsible for lateralized neural responses in linguistic versus spatial processing (Nystrom et al., 2000; Stephan et al., 2003). The distinction between linguistic and spatial functions, however, has typically relied on perceptual characteristics (such as orthographic vs. iconographic), or on broad distinctions, such as sequential versus parallel or global versus local processes (Bradshaw, 1989). Few attempts have been made to compare the two domains with respect to intrinsic, structural properties. From this point of view, NRSD structures offer a unique perspective: they are of biological relevance and universal in natural language grammars and, at least in simple form, they can be transferred symmetrically to the visuo-spatial domain. By adopting such an approach, the present experiment demonstrated that non-rigidly organized stimuli in both the language and the visuo-spatial domain are processed by a common bilateral fronto-parietal network, with an essential contribution of the left IFG. In other words, in the presence of non-rigid dependencies, the processing of spatial information also depends on left hemispheric recruitment, in a qualitatively similar

way to the processing of linguistic information.

The specific role of BA 44 within the IFG for the acquisition of NRSD versus RSD was found to be lateralized to the left hemisphere, independently of the cognitive domain. This indicates that hemispheric specialization may be due to the neural decomposition of intrinsic stimulus features that gives rise to a cohesive spectrum of specialized supramodal higher-order representations (such as for non-rigid versus rigid structures), which may be lateralized to one particular hemisphere. This general principle extends to auditory processing, where the spectrotemporal signal structure is decomposed and differentially processed in the two hemispheres (Boemio et al., 2005), and to visual perception, where the two hemispheres appear to be sensitive each to different sets of visual features (Brown and Kosslyn, 1993). The specific role of the BA 44 within the left IFG for the acquisition of NRSD versus RSD suggests that this brain region may be involved in the computation and acquisition of non-rigid dependencies and, possibly, of non-linear dependencies more in general, independently of the cognitive domain. Accordingly, the activations within the left BA 44 for symbol syntax presented a high degree of anatomical correspondence with those previously found for word syntax, as demonstrated by the small volume correction procedure applied to the different types of analysis that we have reported, with the only exception of the temporal parametric modulation. Even in the latter case, however, both the activations for word and symbol syntax displayed a high probability of being located in BA 44 and, to our knowledge, no further cytoarchitectonic or functional subdivisions for BA 44 have been proposed, yet. At the functional level, the pattern of activity modulation in time within the left BA 44 was comparable for word and symbol syntax, and it is also comparable to a previous study, showing an increase of activation in time within the left BA 44 that was interpreted as a specific correlate of grammatical rule acquisition (Opitz and Friederici, 2003). In addition, our study shows that BA 44 within the left IFG is sensitive to the minimal distinction differentiating NRSD from RSD: in order to elicit a response in this region, this minimal distinction is sufficient and does not need to encompass the full range

of recursive hierarchical phrase structure properties as has been suggested by previous works (Greenfield, 1991; Tettamanti et al., 2002; Musso et al., 2003; Friederici et al., 2006).

Conversely, the right IFG appears to respond to the acquisition of syntactically structured stimuli, independently of the cognitive domain and also independently of whether the syntactic dependencies are rigid or non-rigid. Nevertheless, both the specific overall task effects for symbol-RSD and the analysis of haemodynamic signal modulation induced by learning-related changes in PI show a stronger effect for symbol-RSD versus symbol-NRSD in the right IFG. Since symbol-RSD were more difficult to acquire, these findings may indicate that, while the right IFG responds to any kind of syntactic dependencies, it is sensitive to changes in computational load due to the level of task difficulty. This functional correlate does not seem to be specifically related to the computation of syntactic dependencies, but possibly to explicit search strategies (Fletcher et al. 1999; 2005), such as those required by the judgment of syntactic well-formedness. This is compatible with several previous findings (Tettamanti et al., 2002; Musso et al., 2003; Hoen et al., 2006), and also with the interpretation of activations in the right IFG provided in a previous work by our research group (Moro et al., 2001).

That spoken language is not unique in its dependence upon classical language brain regions, including the left inferior frontal gyrus, is demonstrated for instance by functional neuroimaging research on sign language (Neville et al., 1998; Petitto et al., 2000). Both natural language instantiations are characterized by the use of words, which are assembled in syntactic sequences according to NRSD. Here, using strings of abstract symbols, we show that BA 44 within the left IFG is sensitive to NRSD even in the absence of words, i.e. outside the language domain.

Our results are compatible with the view that BA 44 in the left IFG is characterized by a highly selective capacity to encode NRSD across different modalities. The left IFG, as part of the frontal lobe, is ideally suited for this purpose: supramodal mechanisms are

pervasive within the prefrontal cortex and allow a diverse range of information to be synthesized, processed and stored at an abstract level (Miller, 2000; Duncan, 2001). The left IFG in particular, may be specialized for the analysis, recognition and prediction of non-linear structural relationships within sequential information (such as in the harmonic structure of musical chords (Koelsch, 2005), or in the articulatory orofacial sequences producing speech sounds (Paulesu et al., 2003)). More specifically, it was recently shown that the left IFG is crucially involved in the executive control of hierarchically organized action sequences (Koechlin and Jubault, 2006). The biological salience of these non-linear structural relationships may be a crucial determinant for the recruitment of the left IFG (Schubotz and von Cramon, 2004). We have shown that, with respect to NRSD, the type of information that is encoded in BA 44 within the left IFG can be characterized with a certain degree of accuracy: namely, by disallowing agreement to be established at fixed positions (yielding NRSD, as opposed to RSD structures). The computational burden required by coping with this additional degree of freedom appears to constitute a primary function of BA 44 within the left IFG. Presumably, these computations reflect the prediction and monitoring of syntactic relations over long distances along the speech/word stream (Friederici, 2004). From a complementary perspective, our results show that the need to constrain this degree of freedom, as is the case of RSD, in which position is fixed, as opposed to NRSD, in which position varies freely, leads to longer acquisition times and to an absence of significant activations in BA 44 within the left IFG.

5. CONCLUSIONS

It has been proposed that NRSD are biologically relevant in distinguishing humans from non-human primates. Non-human primates readily learn to master finite state grammars, based on adjacent linear relations, but seem incapable of spontaneously acquiring phrase structure grammars establishing NRSD (Terrace et al., 1979; Jackendoff,

1999; Kuhl, 2000; Fitch and Hauser, 2004; Friederici, 2004). This does not imply that non-human primates could not be taught simple phrase structure grammars by massive training, as suggested by recent findings showing that a species of common songbirds, European starlings, can learn to classify stimuli that are compatible with context-free phrase structure grammars after massive training (Gentner et al., 2006). Spontaneous acquisition of natural language grammars, however, has never been attested in non-human species. This limitation does not appear to be restricted to grammar acquisition: non-human primates lack the capacity to cope with hierarchically organized cognitive processes that give rise to non-rigid sequences of actions, such as in the spontaneous imitation of motor actions (Byrne and Russon, 1998; Conway and Christiansen, 2001; Premack, 2004). Altogether, these observations suggest that the human brain has some distinctive traits by which it is capable of encoding NRSD across diverse higher cognitive functions. Such an encoding process occurs spontaneously by mere exposure to NRSD of great complexity, such as in natural language acquisition. Thus, the ability to encode NRSD may be an essential feature of human behavior. On the other hand, the fact that, under certain circumstances that need to be clarified further, some non-human species can be taught simple NRSD is consistent with the view that language emerged in the course of evolution by drawing on a set of cognitive and computational capabilities that, at least in a rudimentary form, are shared across higher vertebrates. The key issue that needs to be addressed by future research is whether, across species, brain areas homologous to BA 44 within the left IFG in humans subserve these basic computational capabilities, which, as we have shown, underlie both human-unspecific cognitive processes, such as visuo-spatial functions, and human-specific cognitive processes, such as natural language.

6. ACKNOWLEDGEMENTS

Many thanks to Gabriel Baud-Bovy, Vittorio Gallese, Emiliano Macaluso, Alec Marantz and Dorothea Weniger for helpful comments on this manuscript. Supported by the Italian Ministry of University and Research (FIRB 2003119330-009). The authors declare that they have no financial conflicts of interest.

7. REFERENCES

1. Amunts K, Schleicher A, Buergel U, Mohlberg H, Uylings HBM, and Zilles K. Broca's Region Revisited: Cytoarchitecture and Intersubject Variability. *Journal of Comparative Neurology*, 412: 319-341, 1999.
2. Andersson JLR, Hutton C, Ashburner J, Turner R, and Friston K. Modeling Geometric Deformations in EPI Time Series. *Neuroimage*, 13: 903-919, 2001.
3. Boemio A, Fromm S, Braun A, and Poeppel D. Hierarchical and asymmetric temporal sensitivity in human auditory cortices. *Nature Neuroscience*, 8: 389-395, 2005.
4. Bradshaw JL. *Hemispheric Specialization and Psychological Function*. New York: Wiley, 1989.
5. Brown HD and Kosslyn SM. Cerebral lateralization. *Current Opinion in Neurobiology*, 3: 183-186, 1993.
6. Byrne RW and Russon AE. Learning by imitation: a hierarchical approach. *Behavioral and Brain Sciences*, 21: 667-721, 1998.
7. Chomsky N. Three models for the description of language. *IRE Transactions on Information Theory*, 2: 113-124, 1956.
8. Chomsky N. *Syntactic Structures*. The Hague: Mouton, 1957.
9. Chomsky N. *The minimalist program*. Cambridge (MA): MIT Press, 1995.
10. Conway CM and Christiansen MH. Sequential learning in non-human primates. *Trends in Cognitive Sciences*, 5: 539-546, 2001.
11. Dale AM. Optimal Experimental Design for Event-Related fMRI. *Human Brain Mapping*, 8: 109-114, 1999.
12. Dominey PF, Hoen M, Lelekov, and T Blanc JM. Neurological basis of language in sequential cognition: Evidence from simulation, aphasia and ERP studies. *Brain and Language*, 86: 207-225, 2003.
13. Duncan J. An adaptive coding model of neural function in prefrontal cortex. *Nature*

Reviews Neuroscience, 2: 820-829, 2001.

14. Embick D, Marantz A, Miyashita Y, O Neil W, and Sakai KL. A syntactic specialization for Broca's area. *Proceedings of the National Academy of Sciences U.S.A.*, 97: 6150-6154, 2000.
15. Fitch WT and Hauser MD. Computational constraints on syntactic processing in a nonhuman primate. *Science*, 303: 377-380, 2004.
16. Fletcher P, Büchel C, Josephs O, Friston K, and Dolan R. Learning-related neuronal responses in prefrontal cortex studied with functional neuroimaging. *Cerebral Cortex*, 9(2): 168-178, 1999.
17. Fletcher PC, Zafiris O, Frith CD, Honey RA, Corlett PR, Zilles K, and Fink GR. On the benefits of not trying: brain activity and connectivity reflecting the interactions of explicit and implicit sequence learning. *Cerebral Cortex*,15(7): 1002-1015, 2005.
18. Friederici AD. Processing local transitions versus long-distance syntactic hierarchies. *Trends in Cognitive Sciences*, 8: 245-247, 2004.
19. Friederici AD, Bahlmann J, Heim S, Schubotz RI, and Anwander A. The brain differentiates human and non-human grammars: functional localization and structural connectivity. *Proceedings of the National Academy of Sciences U.S.A.*, 103: 2458-2463, 2006.
20. Frison L and Pocock SJ. Repeated measures in clinical trials: Analysis using mean summary statistics and its implications for design. *Statistics in Medicine*, 11: 1685-1704, 1992.
21. Friston KJ, Glaser DE, Henson RN, Kiebel S, Phillips C, and Ashburner J. Classical and Bayesian inference in neuroimaging: applications. *Neuroimage*, 16: 484-512, 2002.
22. Gentner TQ, Fenn KM, Margoliash D, and Nusbaum HC. Recursive syntactic pattern learning by songbirds. *Nature*, 440: 1204-1207, 2006.
23. Greenfield PM. Language, tools and brain: The ontogeny and phylogeny of

hierarchically organized sequential behavior. *Behavioral and Brain Sciences*, 14: 531-595, 1991.

24. Grossman M. A central processor for hierarchically structured material: Evidence from Broca's aphasia. *Neuropsychologia*, 18: 299-308, 1980.
25. Hauser MD, Chomsky N, and Fitch WT. The faculty of language: what is it, who has it, and how did it evolve? Science, 298: 1569-1579, 2002.
26. Henson RN. *Analysis of fMRI time series*. In Frackowiak RSJ, Friston KJ, Frith CD, Dolan R, Price CJ, Zeki S, Ashburner J, and Penny WD (Eds), Human Brain Function. San Diego (CA): Academic Press, 793-822, 2003.
27. Hoen M and Dominey PF. ERP analysis of cognitive sequencing: A left anterior negativity related to structural transformation processing. *Neuroreport*, 11: 3187-3191, 2000.
28. Hoen M, Pachot-Clouard M, Segebarth C, and Dominey PF. When Broca experiences the Janus syndrome: an ER-fMRI study comparing sentence comprehension and cognitive sequence processing. *Cortex*, 42: 605-623, 2006.
29. Hugdahl K and Davidson RJ. *The Asymmetrical Brain*. Cambridge, MA: MIT Press, 2003.
30. Jackendoff R. Possible stages in the evolution of the language capacity. *Trends in Cognitive Sciences*, 3: 272-279, 1999.
31. Koechlin E and Jubault T. Broca's area and the hierarchical organization of human behavior. *Neuron*, 50: 963-974, 2006.
32. Koelsch S. Neural substrates of processing syntax and semantics in music. *Current Opinion in Neurobiology*, 15: 207-212, 2005.
33. Kuhl PK. A new view of language acquisition. *Proceedings of the National Academy of Sciences U.S.A.*, 97: 11850-11857, 2000.
34. Lashley KS. *The problem of serial order in behavior*. In Jeffress LA (Ed), Cerebral mechanisms in behavior: The Hixon Symposium. New York: Wiley, 112-146, 1951.

35. Marcus GF, Vouloumanos A, and Sag IA. Does Broca's play by the rules? *Nature Neuroscience*, 6: 651-652, 2003.

36. Miller EK. The prefrontal cortex and cognitive control. *Nature Reviews Neuroscience*, 1: 59-65, 2000.

37. Moro A, Tettamanti M, Perani D, Donati C, Cappa SF, and Fazio F. Syntax and the brain: disentangling grammar by selective anomalies. *Neuroimage*, 13: 110-118, 2001.

38. Musso M, Moro A, Glauche V, Rijntjes M, Reichenbach J, Buchel C, and Weiller C. Broca's area and the language instinct. *Nature Neuroscience*, 6: 774-781, 2003.

39. Neville HJ, Bavelier D, Corina D, Rauschecker J, Karni A, Lalwani A, Braun A, Clark V, Jezzard P, and Turner. Cerebral organization for language in deaf and hearing subjects: biological constraints and effects of experience. *Proceedings of the National Academy of Sciences U.S.A.*, 95: 922-929, 1998.

40. Nichols T, Brett M, Andersson J, Wager T, and Poline JB. Valid conjunction inference with the minimum statistic. *Neuroimage*, 25: 653-660, 2005.

41. Nystrom LE, Braver TS, Sabb FW, Delgado MR, Noll DC, and Cohen JD. Working memory for letters, shapes, and locations: fMRI evidence against stimulus-based regional organization in human prefrontal cortex. *Neuroimage*, 11: 424-446, 2000.

42. Opitz B and Friederici AD. Interactions of the hippocampal system and the prefrontal cortex in learning language-like rules. *Neuroimage*, 19(4): 1730-1737, 2003.

43. Patel AD. Language, music, syntax and the brain. *Nature Neuroscience*, 6: 674-681, 2003.

44. Paulesu E, Perani D, Blasi V, Silani G, Borghese NA, De Giovanni U, Sensolo S, and Fazio F. A functional-anatomical model for lipreading. *Journal of Neurophysiology*, 90: 2005-2013, 2003.

45. Penny WD and Holmes AP. *Random Effects Analysis*. In Frackowiak RSJ, Friston

KJ, Frith CD, Dolan R, Price CJ, Zeki S, Ashburner J, and Penny WD (Eds), Human Brain Function. San Diego (CA): Academic Press, 843-850, 2003.

46. Petitto LA, Zatorre RJ, Gauna K, Nikelski J, Dostie D, and Evans AC. Speech-like cerebral activity in profoundly deaf people processing signed languages: implications for the neural basis of human language. *Proceedings of the National Academy of Sciences U.S.A.*, 97: 13961-13966, 2000.
47. Premack D. Psychology. Is language the key to human intelligence? *Science*, 303: 318-320, 2004.
48. Schubotz RI and von Cramon DY. Sequences of abstract nonbiological stimuli share ventral premotor cortex with action observation and imagery. *Journal of Neuroscience*, 24: 5467-5474, 2004.
49. Stephan KE, Marshall JC, Friston KJ, Rowe JB, Ritzl A, Zilles K, and Fink GR. Lateralized cognitive processes and lateralized task control in the human brain. *Science*, 301: 384-386, 2003.
50. Terrace HS, Petitto LA, Sanders RJ, and Bever TG. Can an ape create a sentence? *Science*, 206: 891-902, 1979.
51. Tettamanti M, Alkadhi H, Moro A, Perani D, Kollias S, and Weniger D. Neural correlates for the acquisition of natural language syntax. *Neuroimage*, 17: 700-709, 2002.
52. Tettamanti M. *Language Acquisition and Processing: Hierarchically Organized Cognitive Processes*. Ph.D. Thesis. Zurich: Univesity of Zurich, 2003.
53. Tettamanti M and Weniger D. Broca's area: a supramodal hierarchical processor? *Cortex*, 42(4): 491-494, 2006.
54. Van Essen DC, Dickson J, Harwell J, Hanlon D, Anderson CH, and Drury HA. An Integrated Software System for Surface-based Analyses of Cerebral Cortex. *Journal of the American Medical Informatics Association*, 8: 443-459, 2001.

Table 1. Common and specific activations for symbol-NRSD and symbol-RSD

Activations at $p < .05$, FDR corrected for multiple comparisons; § Symbol syntax only (FDR correction over the entire brain volume); ‡ Symbol and word syntax (FDR small volume correction over the voxels activated by word syntax); Z, Z score; k, cluster size; CP, Cytoarchitectonic probabilities (Amunts et al., 1999); a- (prefix), anterior; p- (prefix), posterior; IFG, inferior frontal gyrus; MFG, middle frontal gyrus; medFG, medial frontal gyrus; Ins, insula; CG, cingulate gyrus; IPS, intra-parietal sulcus; IPL, inferior parietal lobule; SPL, superior parietal lobule; Prec, precuneus; IOG, inferior occipital gyrus; MOG, middle occipital gyrus; FusG, fusiform gyrus.

Table 1A. Common activations (conjunction analysis, see Methods)

Area	Z	k	x,y,z	CP	
L aIPS	3.85	42	-46,-38,40		‡
L pIPS	4.14	114	-40,-52,48		‡
L IPL	4.05	"	-30,-56,44		‡
L Prec	4.31	"	-28,-64,48		‡
L IOG	7.45	304	-44,-88,-8		§
L MOG	6.81	"	-46,-70,-16		§
L FusG	5.57	"	-38,-60,-20		§
R/L medFG	5.91	62	0,10,48		‡
R IFG	5.77	66	44,8,24	50% BA44	‡
R IFG	2.92	10	58,14,20	80% BA44	‡
R IFG	3.89	33	48,28,20	30% BA45	‡
R IFG	3.82	"	40,42,12		‡
R MFG	3.79	"	44,38,20		‡
R aIns	4.44	20	32,26,0		‡
R aCG	3.16	18	10,32,24		‡
R aIPS	3.09	13	46,-36,44		‡
R IPL	5.12	239	32,-56,44		‡
R SPL	5.6	"	34,-62,52		‡
R Prec	3.3	"	22,-70,48		‡
R IOG	7.75	508	34,-88,-8		§
R MOG	7.48	"	46,-70,-16		§
R FusG	7.61	"	40,-62,-20		§

Table 1B. Specific activations (interactions, see Methods). The same condition-specific effects were observed when the two conditions were separately compared to the Baseline.

	symbol-NRSD > symbol-RSD				symbol-RSD > symbol-NRSD			
Area	Z	k	x,y,z	CP	Z	k	x,y,z	CP
L IFG	3.61	14	-54,12,24	50% BA44‡				
L IFG					2.43	8	-50,26,4	50% BA45‡
R IFG					3.51	62	48,18,12	20% BA44‡
R IFG					2.47	18	48,30,8	40% BA45‡

Table 2. Non-parametric statistical analysis of behavioral performance index

* Not significant.

a) Kruskal-Wallis test (n=16; 3 tasks x 8 blocks):

Main effect task: $p = 7.711 \times 10^{-12}$

Main effect block: $p = 5.107 \times 10^{-5}$

Interaction task x block: 8.416×10^{-10}

b) Wilcoxon paired tests (n=16; tasks):

symbol-NRSD vs. Baseline: p = .0442

symbol-RSD vs Baseline: $p = 1.15 \times 10^{-11}$

symbol-NRSD vs symbol-RSD: $p = 2.52 \times 10^{-7}$

c) Wilcoxon paired tests (n=16; blocks):

Baseline, block1 vs. block8: p = .0893 *

symbol-NRSD, block1 vs. block8: p = .0115

symbol-RSD, block1 vs. block8: p = .0002

Table 3A. Non-parametric statistical analysis of reaction times

symbol-NRSD: mean RT = 1016 msec, st. dev. = 499

symbol-RSD: mean RT = 1117 msec, st. dev. = 481

Baseline: mean RT = 825 msec, st. dev. = 247

* Not significant.

i) Kruskal-Wallis test (n=16; 3 tasks x 8 blocks):

Main effect task: $p = 1.110 \times 10^{-8}$

Main effect block: p = .0012

Interaction task x block: 1.227×10^{-5}

ii) Wilcoxon paired tests (n=16; tasks):

symbol-NRSD vs. Baseline: p = .0002

symbol-RSD vs Baseline: $p = 3.210 \times 10^{-9}$

symbol-NRSD vs symbol-RSD: p = .0118

iii) Wilcoxon paired tests (n=16; blocks):

Baseline, block1 vs. block8: p = .0562 *

symbol-NRSD, block1 vs. block8: p = .0051

symbol-RSD, block1 vs. block8: p = .0022

Table 3B. Non-parametric statistical analysis of accuracy

symbol-NRSD: mean ACC = 98.61 %, st. dev. = 4.69

symbol-RSD: mean ACC = 94.64 %, st. dev. = 8.69

Baseline: mean ACC = 99.36 %, st. dev. = 1.42

* Not significant.

i) Kruskal-Wallis test (n=16; 3 tasks x 8 blocks):

Main effect task: $p = 1.394 \times 10^{-11}$

Main effect block: p = .0002

Interaction task x block: 3.592×10^{-10}

ii) Wilcoxon paired tests (n=16; tasks):

symbol-NRSD vs. Baseline: p = .7916 *

symbol-RSD vs Baseline: $p = 2.7 \times 10^{-9}$

symbol-NRSD vs symbol-RSD: $p = 1.23 \times 10^{-8}$

iii) Wilcoxon paired tests (n=16; blocks):

Baseline, block1 vs. block8: p = .7500 *

symbol-NRSD, block1 vs. block8: p = .0130

symbol-RSD, block1 vs. block8: p = .0004

FIGURE CAPTIONS

Figure 1. Syntactic dependencies with and without words.

(A) There is no human language where a certain word must occur at a fixed distance from another. Distances between words are specified in terms of relative position and they can always be recursively expanded. So for example, when if occurs in the string, the sentence will contain the word then but the position of the two words cannot be fixed (cf. the underlined words in (i) versus (iii): rigid syntactic dependencies, RSD); rather, it must vary according to the structure and lexical choices of the intermediate words (cf. (i) versus (ii): non-rigid syntactic dependencies, NRSD). **(B)** Syntactic strings made of symbols were construed mimicking both rigid syntactic dependencies (symbol-RSD) and non-rigid syntactic dependencies (symbol-NRSD), as highlighted here for the sake of clarity by the underlined symbols. Symbols are labelled here with their names (k1, k2, ... k10) only for cross-reference with the Materials and Methods section. Underlines and labels did not appear in the actual experiment. Different colors and different sizes (small vs. large) allowed to establish agreement. Stimuli were symmetrically reproducing the contrasts in (A): strings of symbol-NRSD contained concordant elements at varying positions (example strings *NRi*, *NRii*, and *NRiii* following rule symbol-NRSD-1, left), while strings of symbol-RSD contained concordant elements at fixed positions (example strings *Ri*, *Rii*, and *Riii* following rule symbol-RSD-1, right). **(C)** fMRI task design: as exemplified here by rule symbol-NRSD-1, task sessions started with a sample block consisting of only correct (white boxes) strings, followed by a probe block consisting of randomly intermixed correct and incorrect (grey boxes) strings. As shown in the right frame, string presentation terminated by button press, after which a feedback indicating right or wrong answer appeared, followed by a variable time interval.

Figure 2. Rule type effects for word syntax versus symbol syntax

Areas of activation ($p < .05$, FDR corrected for multiple comparisons) are displayed on cortical renderings of the participants' average anatomical image. **(A)** The areas of conjoined activation between symbol-NRSD and symbol-RSD in acquisition of symbol syntax only are shown in blue; the areas of conjoined activation between symbol-NRSD and symbol-RSD which overlap with word syntax are shown in yellow. The areas of conjoined activations between word-NRSD and word-RSD are reported for reference in **(B)** (for details, see Tettamanti et al., 2002). **(C)** Areas of activation ($p < .05$, FDR corrected for multiple comparisons) specific for symbol-NRSD (in red) and for symbol-RSD (in green) are displayed on flat cortical maps. An arrow links the *pars opercularis* of the left IFG with the corresponding average post-stimulus percent signal changes in symbol-NRSD and symbol-RSD, with respect to whole-brain mean; plot bars represent percent signal change every 3 seconds post-stimulus time bin; pink bars represent 90% confidence intervals. Cis, cingulate sulcus; CS, central sulcus, IPS, intra-parietal sulcus; SF, sylvian fissure; SFS, superior frontal sulcus; STS, superior temporal sulcus. **(D)** Cytoarchitectonic probability of activations in the left IFG. Areas of activation ($p < .05$, FDR corrected for multiple comparisons) in the left IFG specific for symbol-NRSD (in red) and for symbol-RSD (in green) are rendered on the participants' average flat cortical map of the left hemisphere. The areas of activation are superimposed on cytoarchitectonic probability maps (Amunts et al., 1999) (rose-violet color scale) for BA 44 (left) and BA 45 (right).

Figure 3. Temporal modulations in the left IFG.

(A) Significant modulation in time during fMRI scanning sessions ($p < .05$, FDR corrected for multiple comparisons) in the left IFG for symbol-NRSD. Arrows link the *pars opercularis* of the left IFG with: **(B)** Depiction of temporal parametric modulation of haemodynamic response across scan time (average scan time across subjects) in this brain region. Effects are expressed as percent signal changes, with respect to whole-brain

mean. Left, modulations for symbol-NRSD; right, modulations for symbol-RSD. Note the higher absolute range of percent signal change for symbol-NRSD versus symbol-RSD, as represented by orange versus green color scales, corresponding to a stronger modulation in time in the left IFG.

Figure 4. Modulation by performance in the left IFG.

(A) Areas of activation significantly modulated by performance ($p < .05$, FDR corrected for multiple comparisons) are displayed on cortical renderings of the participants' average anatomical image. These were, in red, for symbol-NRSD, the left IFG, and, in green, for symbol-RSD, the right IFG. Arrows link the *pars opercularis* of the left IFG with: **(B)** Depiction of parametric modulation of haemodynamic response by performance index (PI), averaged across subjects, in this brain region. Effects are expressed as percent signal changes, with respect to whole-brain mean. Left, modulations for symbol-NRSD; right, modulations for symbol-RSD. Note the higher absolute range of percent signal change for symbol-NRSD versus symbol-RSD, as represented by the orange versus green color scales, reflecting a stronger modulation of the left IFG by PI. **(C)** Plot of behavioral PI across task duration for the baseline condition (gray), symbol-NRSD (orange), and symbol-RSD (green). Vertical bars represent lower standard deviation ranges (see Table 2, for the statistical analysis of behavioral data).

Figure 1

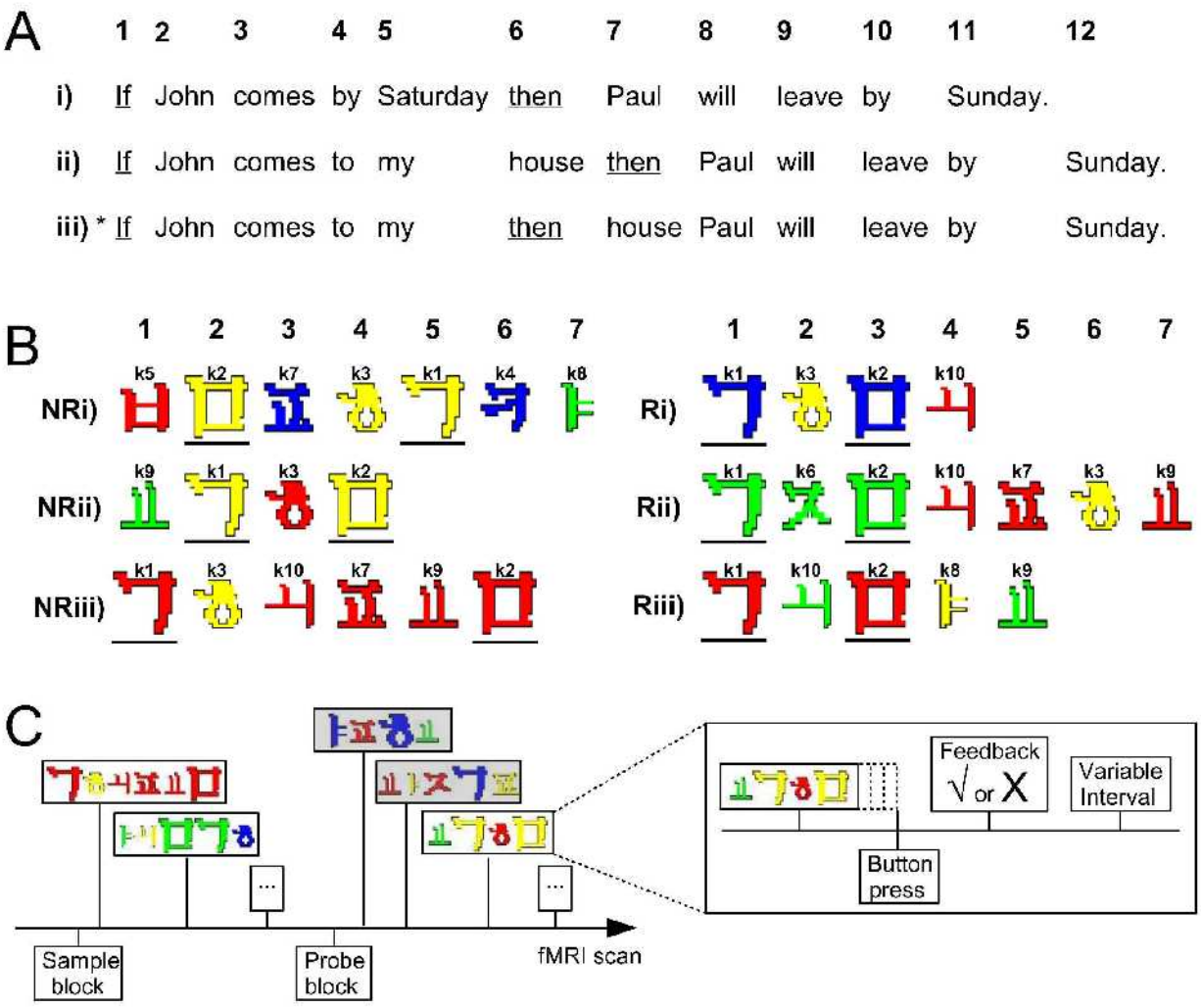
A
1 2 3 4 5 6 7 8 9 10 11 12
i) If John comes by Saturday then Paul will leave by Sunday.
ii) If John comes to my house then Paul will leave by Sunday.
iii) * If John comes to my then house Paul will leave by Sunday.
B
1 2 3 4 5 6 7
NRi)
NRii)
NRiii)
Ri)
Rii)
Riii)
C
Sample block
Probe block
fMRI scan
Feedback
√ or X
Variable Interval
Button press

Figure 2

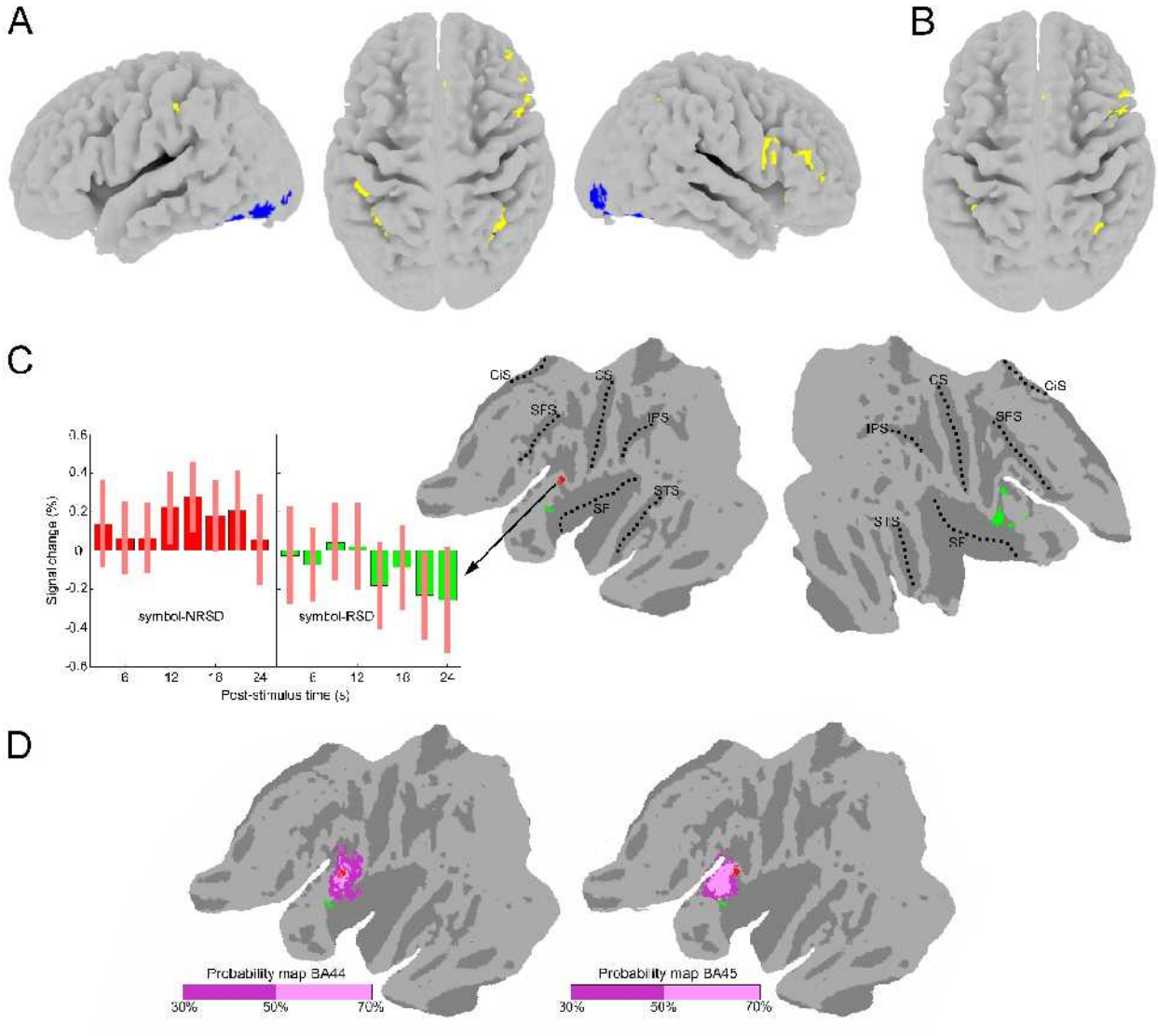
A
B
C
CiS
CS
SFS
IPS
STS
SF
Signal change (%)
symbol-NRSD
symbol-RSD
Post-stimulus time (s)
D
Probability map BA44
30%
50%
70%
Probability map BA45
30%
50%
70%

Figure 3

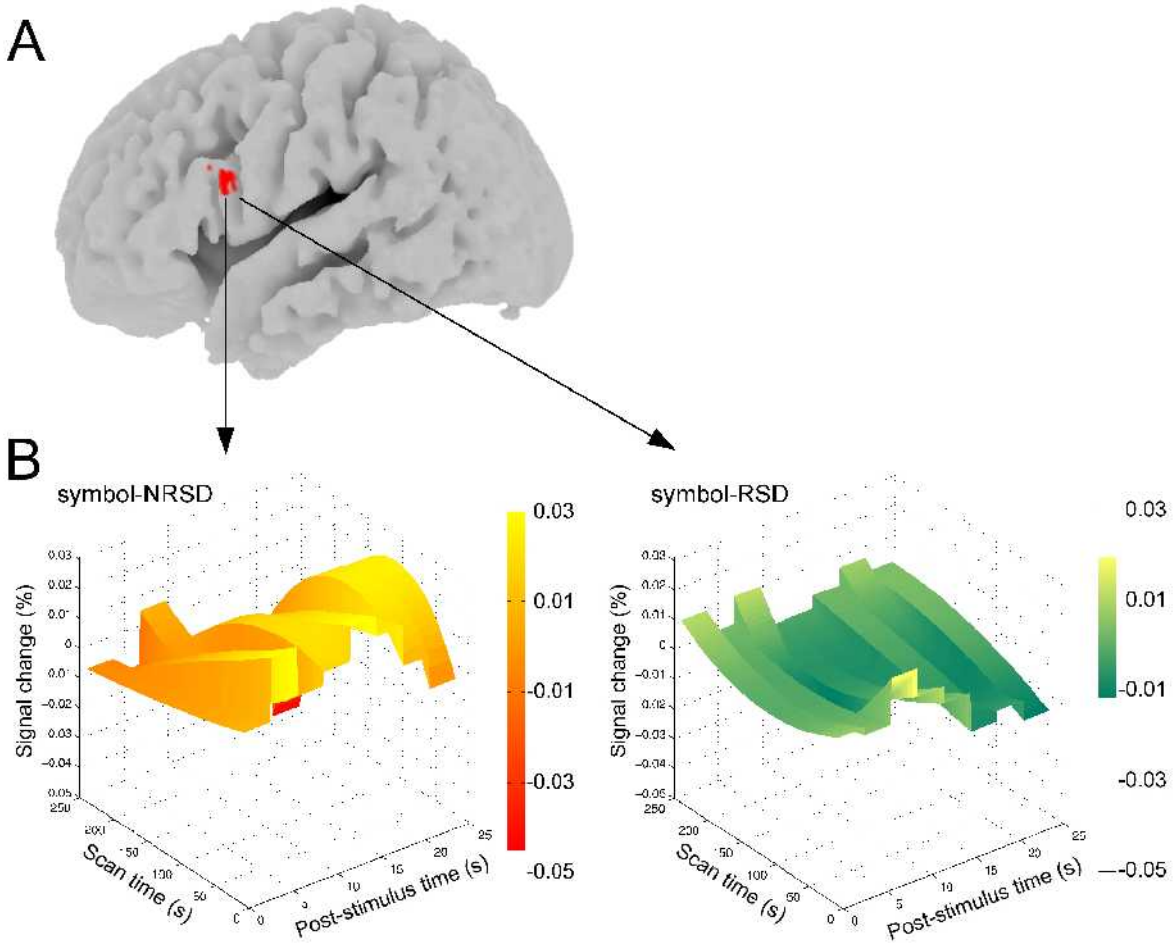
A
B
symbol-NRSD
symbol-RSD
Signal change (%)
Scan time (s)
Post-stimulus time (s)
0.03
0.01
-0.01
-0.03
-0.05

Figure 4

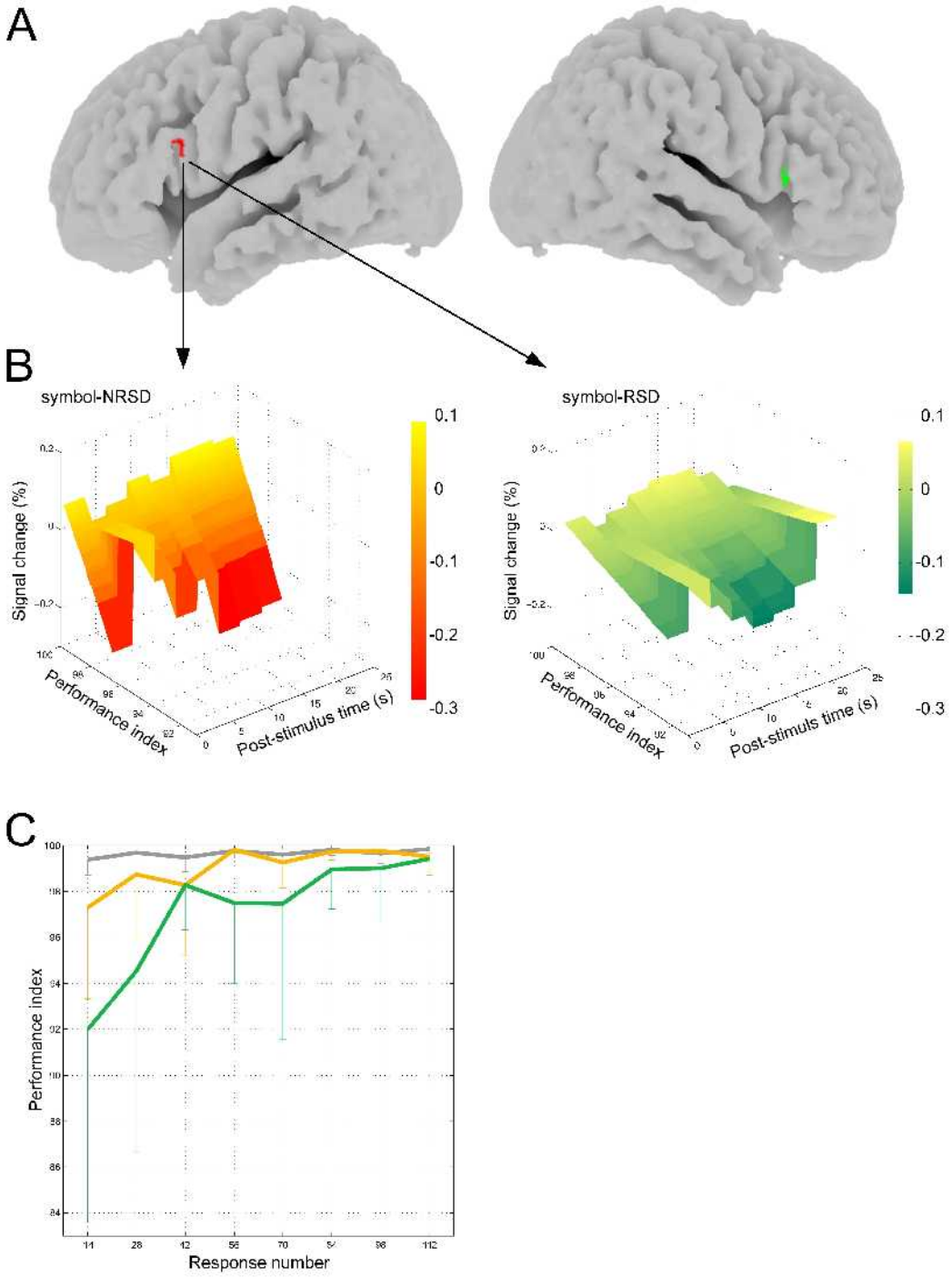
A
B
symbol-NRSD
symbol-RSD
Signal change (%)
Performance index
Post-stimulus time (s)
0.1
0
-0.1
-0.2
-0.3
C
Performance index
Response number